SUPPORTING INFORMATION

Transferring axial molecular chirality through a sequence of on-surface reactions

Néstor Merino-Díez[1,2,3,‡], Mohammed S. G. Mohammed[1,3,‡], Jesús Castro-Esteban[4,‡], Luciano Colazzo[1,3], Alejandro Berdonces-Layunta[1,3], James Lawrence[1,3], J. Ignacio Pascual[2,5], Dimas G. de Oteyza[1,3,5,*] and Diego Peña[4,*]

1. Donostia International Physics Center (DIPC); 20018 San Sebastián, Spain.

2. CIC nanoGUNE, nanoscience cooperative research center; 20018 San Sebastián, Spain.

3. Centro de Física de Materiales-Material Physics Center (CFM-PCM), 20018 San Sebastián, Spain.

4. CiQUS, Centro Singular de Investigación en Química Biolóxica e Materiais Moleculares; 15705 Santiago de Compostela, Spain.

5. Ikerbasque, Basque Foundation for Science; 20018 San Sebastián, Spain.

email: d_g_oteyza@ehu.es; diego.pena@usc.es

Table of Contents

EXPERIMENTAL METHODS

Sample preparation. 2,2'-Dibromo-9,9'-bianthracene (DBBA) was synthesized following the procedure previously described.[1] The enantiomers of DBBA were separated by HPLC (Agilent 1200) equipped with a chiral semipreparative column (Lux immobilized amylose-1; 4.6 x 250 mm, 5 μm). The racemic mixture was separated using hexane:iPrOH (99:1) with a flow rate of 1.8 mL/min at 298 K (Fig S2). The optical rotations of each enantiomer were recorded on a JASCO P-2000 Polarimeter at 296 K using a sodium lamp (589 nm), obtaining a value of $[\alpha]_D = -47.26$ (c = 0.003, CH_2Cl_2) for the first HPLC peak and $[\alpha]_D = +46.07$ (c = 0.002, CH_2Cl_2) for the second HPLC peak. For the preparation of the different samples, the enantiomers of DBBA were independently evaporated at 435 K from a home-made Knudsen cell oriented towards the monocrystalline Au(111) surface substrate for deposition. Atomically cleaned Au(111) surface were obtained by standard sputtering (0.8 kV, Ar^+) and annealing cycles (705K). Thermally-induced on-surface reactions were performed by radiative heating, at 415K (525K) for Ullmann coupling (cyclodehydrogenation).

STM imaging and analysis. Sample analysis was performed in a commercial Scienta-Omicron low-temperature STM under ultrahigh vacuum (UHV) conditions with pressure values below the 10^{-10} mbar range and a base temperature of 4.3 K. All STM images were processed with the WSxM software.[2] The chirality determination from the STM images was performed as described in the text, and the provided statistics are the result of counting the number of monomer units (each accounting for one unit cell in polymers and GNRs) observed in polymers or GNRs of each handedness. For larger scale images, once the chirality of a polymer or GNR is determined, the number of monomers is estimated from the polymer/GNR length divided by the respective unit cell size. The reported errors stem from the square root of the total monomer counts for each species and chirality. The total number of monomers considered in the statistics amount to 7200, 2077 and 2150 in the samples corresponding to the enantioenriched S-reactants in the

polymer phase, enantioenriched S-reactants in GNR phase, and the control experiment with enantioenriched R-reactants in GNR phase, respectively.

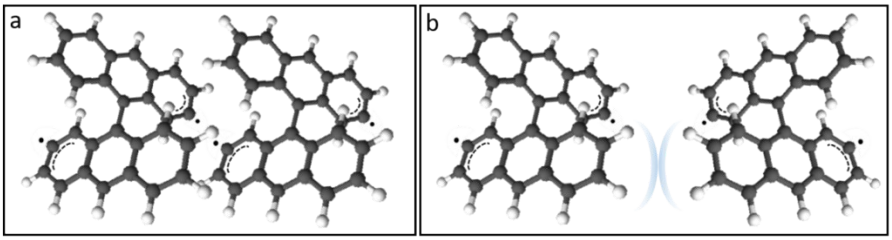

Fig. S1. 3D models illustrating the steric hindrance exerted between dehalogenated monomers of (a) the same and (b) different chirality. The latter displays a strong steric hindrance that hinders polymerization of monomers with opposite chirality.

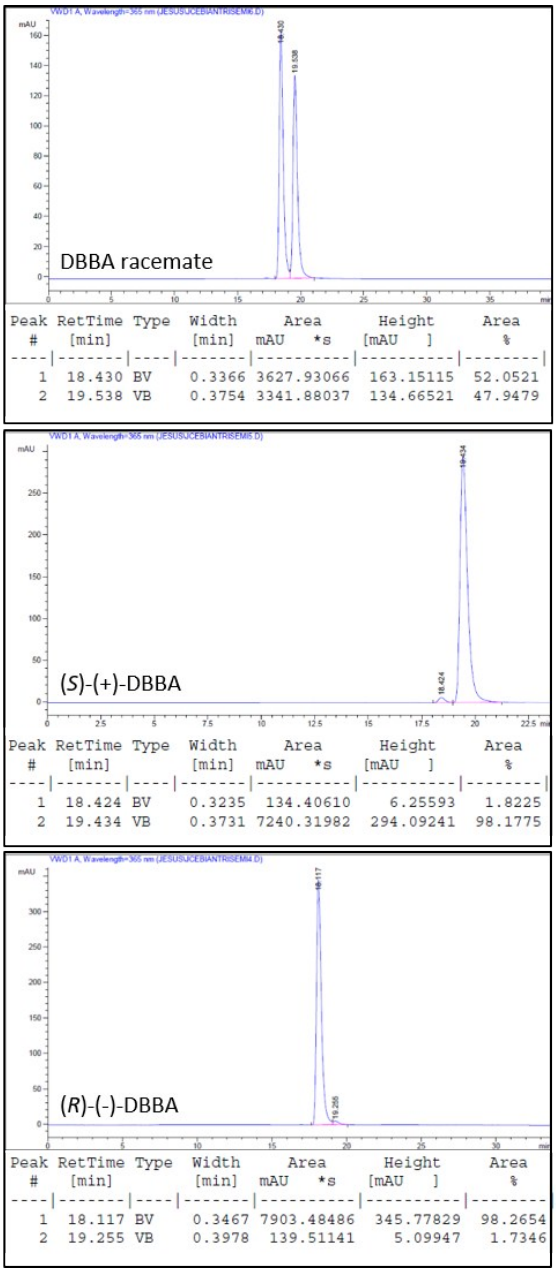

Peak #	RetTime [min]	Type	Width [min]	Area mAU *s	Height [mAU]	Area %
1	18.430	BV	0.3366	3627.93066	163.15115	52.0521
2	19.538	VB	0.3754	3341.88037	134.66521	47.9479

Peak #	RetTime [min]	Type	Width [min]	Area mAU *s	Height [mAU]	Area %
1	18.424	BV	0.3235	134.40610	6.25593	1.8225
2	19.434	VB	0.3731	7240.31982	294.09241	98.1775

Peak #	RetTime [min]	Type	Width [min]	Area mAU *s	Height [mAU]	Area %
1	18.117	BV	0.3467	7903.48486	345.77829	98.2654
2	19.255	VB	0.3978	139.51141	5.09947	1.7346

Fig. S2. Chiral HPLC profiles for (top) DBBA racemate, and enantiomerically enriched (middle) (*S*)-(+)- and (bottom) (*R*)-(-)-DBBA precursors.

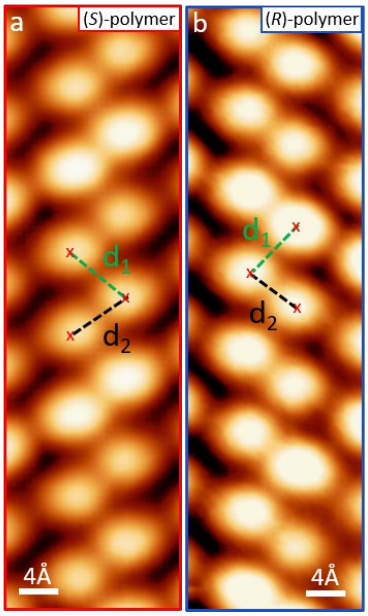

Fig. S3. Identification of the polymer's chirality from their non-equivalent intramolecular distances between the uppointing ends of the tilted anthracene moieties. Examples (a) (S)-polymer and (b) (R)-polymer (Vs = 0.5 V, It = 10-50 pA).

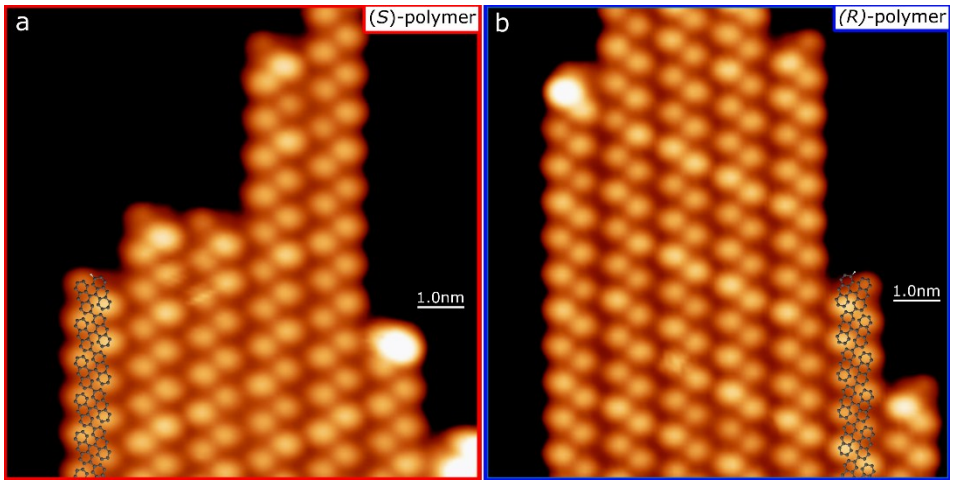

Fig. S4. Identification of the polymer's chirality from their longitudinal end oblique orientation. Examples (V_s = 0.5 V, I_t = 50 pA) of (a) (*S*)-polymer and (b) (*R*)-polymer with superimposed models where, for an easier visualization, just terminal hydrogen atoms (in white) are represented.

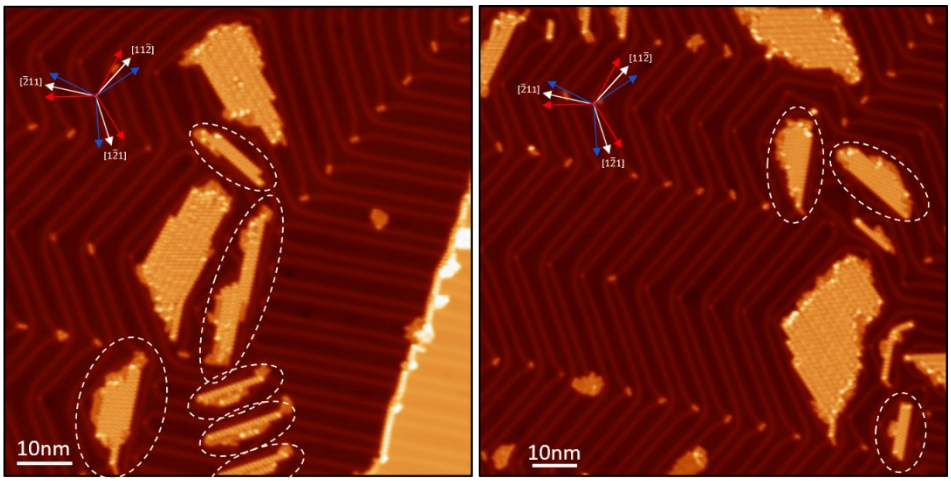

Fig. S5. STM images (V_s = 1.0 V, I_t = 32 pA) showing examples of (*S*)-polymers islands out of main growth orientations (circled in white dashed lines).

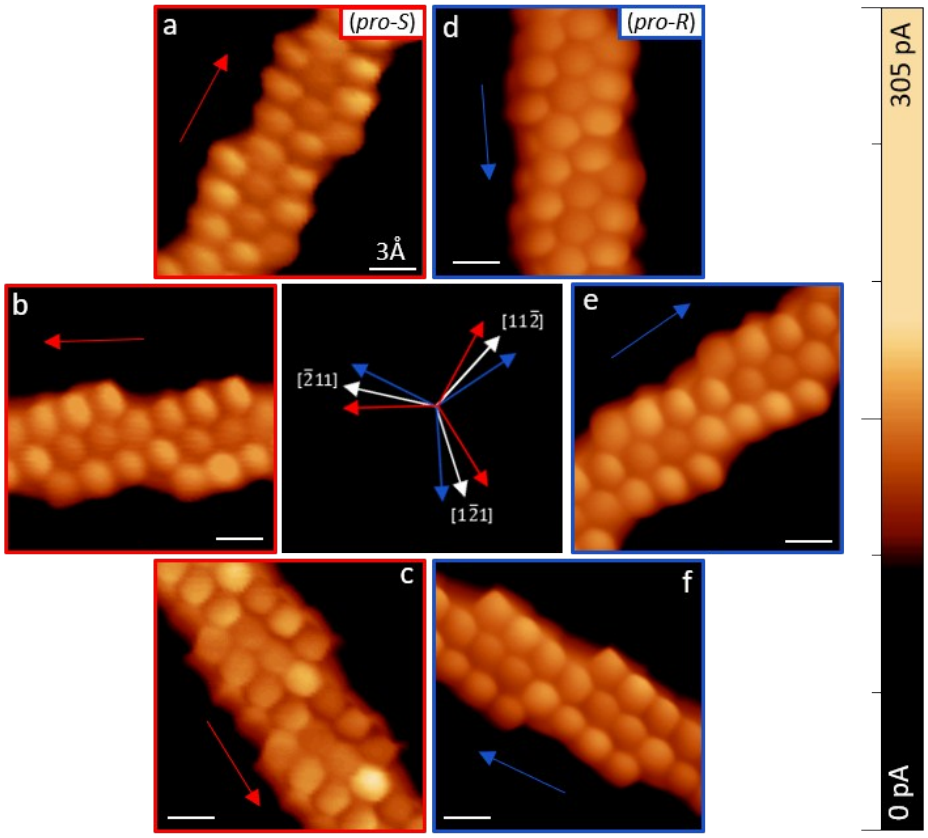

Fig. S6. Constant-height current maps (U_s = 2 mV, color scale on the right) with a CO-terminated tip showing (a-c) (*pro-S*)-GNRs and (d-f) (*pro-R*)-GNRs in their three growth orientations on Au(111), as indicated in the central inset.

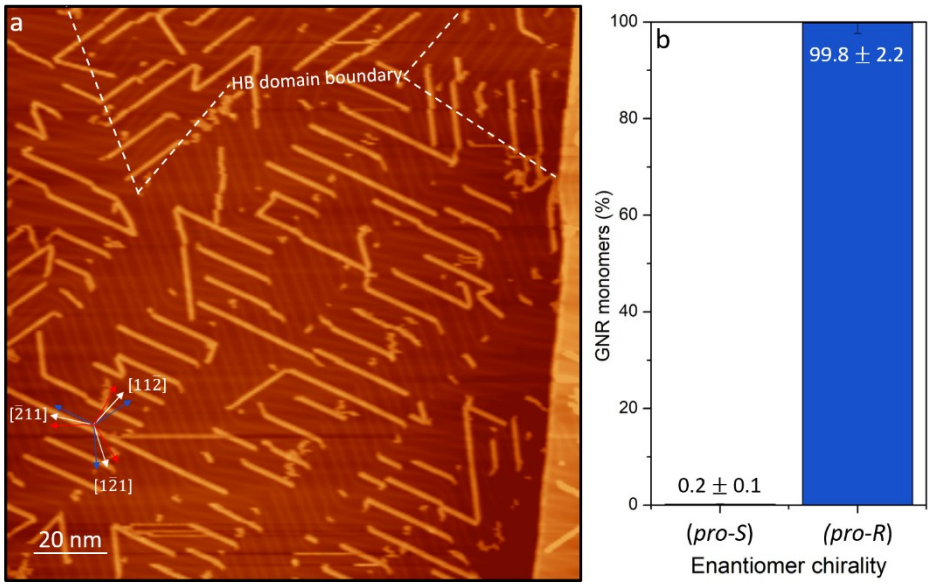

Fig. S7. a) Representative STM overview image (V_s = 0.1 V, I_t = 50 pA) of the sample after depositing enantioenriched (*R*)-(-)-DBBA precursor and inducing its polymerization and cyclodehydrogenation. White dashed lines represent the boundaries of the herringbone reconstruction domains that determine the preferred orientations of GNRs. Inset indicates the preferred adsoption orientations of prochiral GNRs with respect to Au(111) . b) Enantiomeric distribution of the monomers forming the GNRs after polymerization and cyclodehydrogenation of enantioenriched (*R*)-(-)-DBBA precursors.

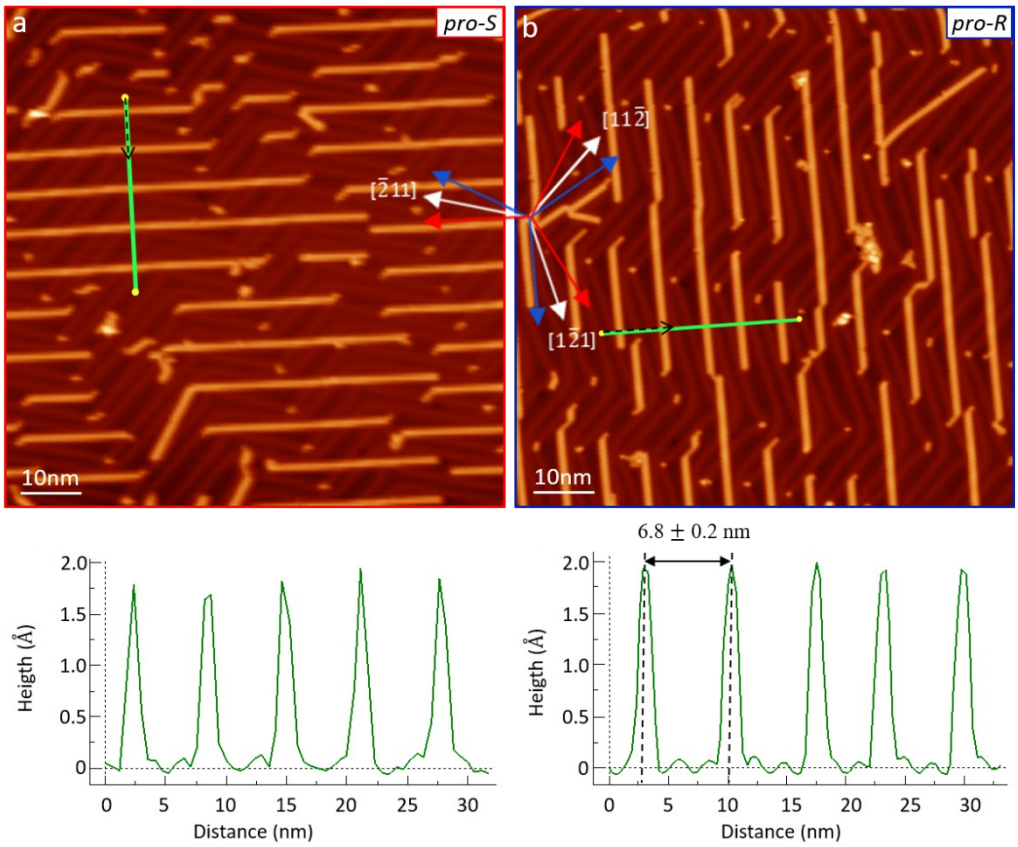

Fig. S8. STM images (V_s = 1.0V, I_t = 200pA; V_s = 0.5V, I_t = 150pA) showing the well-defined preferred interspacing observed for both (a) (*pro-S*)-GNRs and (b) (*pro-R*)-GNRs. Green lines correspond to the height profiles at the bottom of each image. Dashed black lines indicate the height profile directions.

References

[1] D. G. de Oteyza, A. García-Lekue, M. Vilas-Varela, N. Merino-Díez, E. Carbonell-Sanromà, M. Corso, G. Vasseur, C. Rogero, E. Guitián, J. I. Pascual, et al., *ACS Nano* **2016**, *10*, 9000–9008.

[2] I. Horcas, R. Fernández, J. M. Gómez-Rodríguez, J. Colchero, J. Gómez-Herrero, A. M. Baro, WSXM: A Software for Scanning Probe Microscopy and a Tool for Nanotechnology. *Rev. Sci. Instrum.* **2007**, *78*, 013705